Nanoscale

The Molecular Basis of Interaction Domains of full-length PrP with Lipid Membrane

Journal:	*Nanoscale*
Manuscript ID	NR-COM-03-2019-002735.R1
Article Type:	Communication
Date Submitted by the Author:	09-May-2019
Complete List of Authors:	Pan, Yangang; University of Nebraska Medical Center College of Pharmacy, Department of Pharmaceutial sciences Wang, Bin; University of Georgia, College of Engineering Reese, Alexander ; University of Georgia, College of Engineering Xu, Bingqian; University of Georgia, College of Engineering

COMMUNICATION

The Molecular Basis of Interaction Domains of full-length PrP with Lipid Membrane

Received 00th January 20xx,
Accepted 00th January 20xx

DOI: 10.1039/x0xx00000x

Yangang Pan,[a,b] Bin Wang, [a,c] R Alexander Reese, [a] and Bingqian Xu [a,*]

PrP-lipid membrane interactions are critical to PrP structure conversion and neurotoxicity, but its molecular mechnism remains unclear. Two-dimensional histogram of force-distance curves and worm-like chain model revealed three binding regions at PrP N-terminal, providing the molecular basis for understanding the interactions between full-length PrP and lipid membranes.

Introduction

Prion diseases or transmissible spongiform encephalopathies are a set of fatal neurodegenerative diseases that include scrapie, bovine spongiform encephalopathy, and Creutzfeldt-Jakob disease[1]. They are chiefly characterized by the misfolding of the normal form of the prion protein (PrPC) into protease-resistant β-sheet-rich conformers (PrPSc), which may form insoluble cytotoxic aggregates and show a remarkable resistance to proteolytic digestion[2-5]. These aggregates are associated with a wide range of neurodegenerative diseases[6, 7]. It remains experimentally challenging to precisely elucidate the early stages of the aggregation process, wherein heterogeneous oligomers organize into the larger, disease-causing fibrils[8]. This aggregation process is believed to be similar to that of the aggregation processes of amyloid beta (Aβ), tau, and α-synuclein, which lead to various neurodegenerative diseases in humans[9, 10]. Therefore, greater understanding of theses aggregation processes in prion diseases will lead to more effective treatments of the various diseases associated with proteinaceous aggregations.

With fluorescence quenching and circular dichroism (CD) spectroscopy, the full-length PrP(23-231) has been shown to possess binding capacity to non-detergent-resistant microdomains (DRM), specifically to the anionic phospholipid at low pH[11]. Great efforts have been made to prove that the lipid membrane binding is related to the structure and conformation change of PrP[11-14]. PrP-lipid interactions have been suggested as relating to prion-induced neurotoxicity[15] and normal physiological functions[16-18]. Similar findings have been made on Aβ-lipid interactions as well[10, 19]. In order to investigate the possible biological relevance of such interactions, full-length PrP and lipid membrane interaction details, such as the precise lipid interaction sites on PrP molecule and the corresponding interaction forces, need to be investigated.

According to structural features, PrP can be divided into an unstructured N-terminal fragment (residues 23-124), and a structured C-terminal domain[20-22]. Previous studies suggest that the N-terminal of PrP has high affinity toward lipid bilayer[11, 23, 24]. Different PrP fragments were used to investigate the precise determinants in binding of N-terminal to lipid membrane. By using CD spectroscopy and fluorescence spectroscopy, researchers showed that the synthetic peptide related to the PrP tetra-octarepeat region can bind to micelles through insertion of the tryptophan residues into the acyl chain region of the membrane[25]. To model the binding affinity of the N-terminal subdomains to lipid membrane, the lipid membrane binding ability of PrP fragments PrP(23-50), PrP(23-89), PrP(23-110), PrP(23-110), PrP(50-110), PrP(51-89), and PrP(90-110) were investigated by bulk methods, including quartz crystal microbalance with dissipation, fluorescence spectroscopy, and solid-state NMR[26]. In this study only PrP(23-89) and PrP(23-110) interact with lipid membrane, which suggests that the combination of different subdomains is needed for effective membrane interaction. Recently, CD spectroscopic measurements have shown that the amyloid formation of PrP(106–126) is mediated by membrane[27].

Although the binding fragments of PrP to lipid membrane has been widely studied as discussed above, several issues remain: (i) PrP fragments could form aggregates in the solution, which would affect the PrP lipid interactions; (ii) the lipid-interacting regions in full-length PrP is ill-defined; and (iii) the information regarding the dynamic behaviors of full-length PrP-lipid interactions at the single-molecule level cannot be acquired by bulk methods. Supported lipid bilayers (SLBs) are used to mimic the cell membrane with high stability and accessibility, which is suitable for various measurement techniques[28]. Here, we investigated the dynamic interactions between full-length

[a] *Single Molecule Study Lab., College of Engineering, University of Georgia, Athens, GA 30602, USA, E-mail:.bxu@engr.uga.edu*
[b] *Department of Pharmaceutical Sciences, University of Nebraska, Omaha, NE 68195, USA*
[c] *United States Department of Agriculture, Agricultural Research Service, National Poultry Research Canter, Athens ,GA 30605, USA*

† Electronic Supplementary Information (ESI) available: See DOI: 10.1039/x0xx00000x

PrP and SLBs with single-molecule force spectroscopy (SMFS). Single-molecule manipulation has key advantages in studying dynamic interactions. By taking many highly-sensitive sequential measurements, dynamic and statistical information on multiple, discrete binding events, including the distribution of events in inhomogeneous systems can be gleaned[29]. Such information can be lost through common bulk solution methods, which measure an ensemble of molecular states. In the present system, SMFS can be applied by precisely attaching to a gold-coated atomic force microscopy (AFM) tip via an exposed disulfide. From the collected data, the force-distance two-dimensional histogram of the unbinding events and the worm-like chain simulation elucidate the exact lipid-interacting regions in PrP molecule.

Results and discussion

Frozen full-length human recombinant prion protein (sequence: 23-231, theoretical PI/Mw: 9.39/23571.92) was purchased from Calbiochem® in Germany with a concentration of 2mg/mL, which was from E. coli expression and purified as previously described[42]. The purity of >95% was determined by SDS-PAGE. The protein was stored at -20 °C in 10 mM sodium acetate buffer at pH 4.0 before usage. Before each experiment, purchased prion protein was centrifuged (20000g) for 30 min at 4°C to remove pre-existing aggregates. The three-dimensional structure of full-length PrP at pH 5.0 is simulated by Amber 11, with 60 ns equilibration and the results are shown in Figure 1. The experimental details of the structure simulations, AFM tip modification, and supported lipid bilayers are illustrated in Figure S1 (ESI S1†).

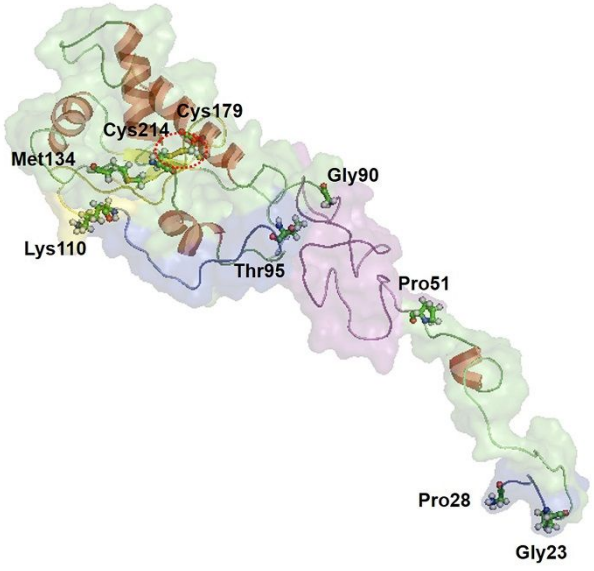

Fig. 1 The simulated structure of the PrP, with the important fragments labelled by the boundary amino acids, including CC1 (Gly23 to Pro28), OR (Pro51 to Gly90), CC2 (Thr95 to Lys110), HD (Lys110 to Met134), and the disulfide bond formed by Cys179 and Cys214.

The dynamic simulations show that the C-terminal domain of PrP is structured and the N-terminal (23-124) is unstructured, which is consistent with previous studies[20, 21]. Additionally, the simulations confirm previous reports[21, 22] that the residues Cys179 and Cys214 are exposed and that they form a disulfide bond at pH 5.0, as shown in Figure 1 (red ring). The sulfur atoms from the two cysteine residues form the disulfide bond of PrP, and the two Au-S bonds to the gold film on the AFM tip. Our previous study suggests that PrP proteins form clear parallel patterns along reconstructed gold (111) surface through Au-S bonds[30]. The Au-S bond is stronger than any non-covalent bond. Therefore, it can be used to fix the orientation of the full length PrP molecule so that the unbinding event can only happen between the PrP N-terminal and the lipid membrane via the non-covalent interactions. In this particular study, in order to further determine whether the sulfur atoms from the disulfide bond in the protein have a strong interaction with Au, the AFM tip was modified with PrP through two methods: (i) Covalent attachment of an exposed primary amine of PrP to the gold-coated AFM tip via a heterobifunctional linker and EDC/NHS coupling, as shown in Figure 2A and (ii) direct immersion of the gold-coated AFM tip into a solution of PrP at pH 4.5, as illustrated in Figure 2C. Force curves for each condition were then recorded between the modified AFM tip and a bare gold surface (Figure 2B and 2D). Force-distance curves were acquired using the AFM 5500 (Agilent Technologies, Chandler, AZ) in 10 mM sodium acetate. The spring constant of the AFM tip were determined according to the thermal noise method. The average spring constant was about 0.03 N/m. The loading rate is ~30 nN/s.

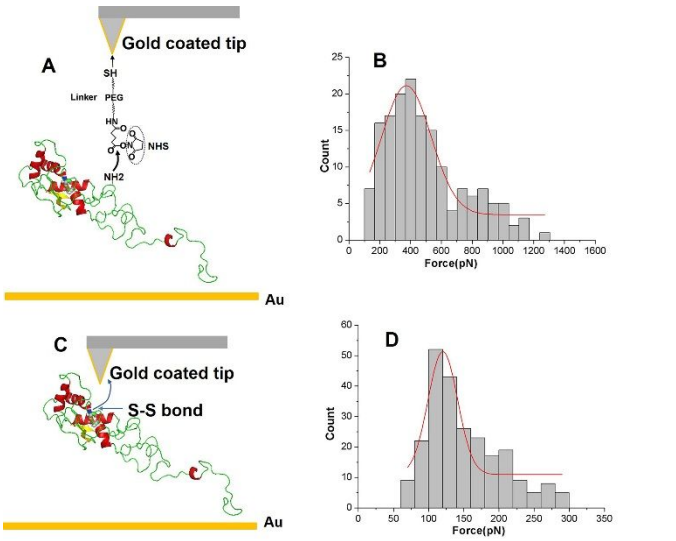

Fig. 2 Force spectroscopy on bare gold. (A) Scheme for PrP conjugation to the AFM tip via a heterobifunctional PEG linker. (B) Distribution of rupture force corresponding the modification methods as shown in Figure 1A. (C) Scheme for PrP conjugation to the AFM tip via the formation of a covalent bond between the gold-coated tip and an exposed disulfide on PrP formed from residues Cys179 and Cys214. (D) Distribution of rupture force corresponding to the modification methods as shown in Figure 1C.

For the heterobifunctional linker method, the most probable rupture force was 378.2 ± 14.5 pN (Figure 2B). The direct immersion method produced a most probable rupture force of

120.2 ± 3.6 pN (Figure 2D). Single molecule force spectroscopy has been proven to be capable of real-time observation of distinct bond states[31].

In our study, different unbinding forces are acquired corresponding to two modification methods, which suggests that the PrP is modified on the gold coated AFM tip though the sulfur atoms from the disulfide bond. This functionalization scheme permits controlled attachment of the PrP to the AFM tip at the site of the disulfide on the C-terminal, preserving freedom for the N-terminal to interact with lipid membrane.

The tips functionalized via direct immersion were used to perform force-distance curves on the lipid membrane containing the anionic phospholipid 1-palmitoyl-2-oleoyl-sn-glycero-3-phosphocholine (POPS) and the zwitterionic phospholipid 1-palmitoyl-2-oleoyl-sn-glycero-3 phosphocholine (POPC), which are the two predominant phospholipids comprising neuronal cell membranes, as shown in Figure 3A[32]. Figure 3B shows representative force-distance curves of different unbinding distances. Three peaks at unbinding distances 11.6 ± 0.1 nm, 20.1 ± 0.2 nm, and 34.3 ± 0.4 nm were obtained (Figure 3C).

Unbinding distances have been previously used for revealing the DNA methylation pattern by Zhu and coworkers[33]. In our work, the different distribution of unbinding distances suggests that the PrP has three binding regions with the lipid membrane.

PrP was attached to the AFM tip though Cys179 and Cys214. Based on the structure of PrP, if the α/β loop was stretched, the unbinding distance of around 4.85.3 nm or 14.7 nm should be detected. These distance values is are calculated from ΔL=n×l-dT, where dT is the distance between the terminals of the structured domain, l is the contour length per amino acid, and n is the number of amino acids between the two β sheets (Met134 and Tyr163) and Cys179. Given dT ≈ 0.5 nm or 1.5 nm from the simulated structure (ESI Figure S2 †), the crystallographic value l= 0.36 nm and n=16 or 45 counted from the structure of PrP.

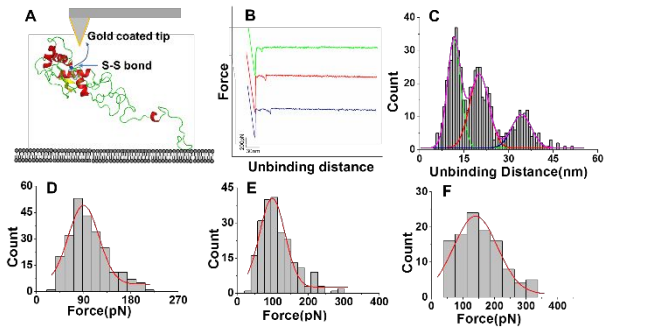

Fig. 3 Force spectroscopy on lipid membrane. (A) Scheme for PrP conjugation to the AFM. (B) Representative force-distance curves between a PrP-modified tip and lipid membrane. (C) The distribution of unbinding distance. (D) The distribution of force corresponding to unbinding distance at Peak 1. (E) The distribution of force corresponding to unbinding distance at Peak 2. (F) The distribution of force corresponding to unbinding distance at Peak 3.

However, in our experiments, these two unbinding distance were not detected as the most probable distance value. In addition, the force of unfolding an α/β protein at a loading rate of 6 nN/s is about 68 pN and the slope of force-loading rate curve is about 8.9×10^{-3} s, as shown by He and coworkers[34]. It is will be more than 250 pN while unfolding the α/β protein structure at ~30 nN/s. However, at this loading rate, the rupture forces at 89.7±2.7 pN (Figure 3D), 98.7±3.0 pN (Figure 3E), and 139.7±8.7 pN (Figure 2F) were detected. These data indicate that the α/β loop was not stretched in our experiments. The force-extension curves of protein have been most appropriately described by the extended worm-like chain (WLC) model (ESI Eq. S1 †)[35, 36]. Briefly, the extension of the protein is related to the stretching force. Therefore, we plot the force-distance two-dimensional histogram to reflect the frequency distribution of given pairings of force and unbinding distance. It has been suggested that the N-terminal of PrP is divisible into four consecutive domains, a first charge cluster (CC1: Gly23 to Pro28), a second charge cluster (CC2: Thr95 to Lys110), the octapeptide repeat (OR: Pro51 to Gly90), and a hydrophobic domain (HD: Lys110 to Met134)[37], as shown in Figure 4A. Due to the different cleavage residues, PrP generates N1 (23–110) and N2 (23-89) fragments[38, 39]. WLC simulation curves of different parts of PrP were conducted for data analysis. Combining the force-distance two-dimensional histogram and WLC simulation curves, it is clearly shown that the binding regions we detected are located at CC2, OR and PrP(23-51), as shown in Figure 4B. The exact lipid-interacting regions in PrP are well-defined, which indicates that combining the force-distance two-dimensional histogram with WLC simulation curves is an accurate method to define the binding sites.

Because the force-distance curves have high resolution in distinguishing the unbinding distances[33], if there are the PrP molecule has three lipid-membrane binding regions in PrP, two or three unbinding events should be detected in one force curve simultaneously. As expected, these kinds of force distance curves were observed. By analyzing the stretching distance, four kinds of force-distance profiles were categorized: (i) The regions of CC2 and OR bind to lipid membrane (Figure 4C i); (ii) CC2 and PrP(23-51) bind to lipid membrane (Figure 4C ii); (iii) OR and

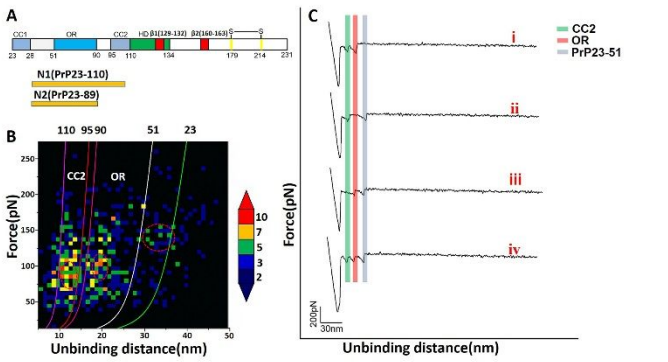

Fig. 4 Force spectroscopy analysis. (A) Diagram of the full-length PrP structure. (B) Force– distance two-dimensional histogram. The lines represent worm-like chain (WLC) fits. (C) Representative force-distance curves with two or three unbinding events that are detected in one force curve simultaneously.

PrP(23-51) bind to lipid membrane (Figure 4C iii); (iv) CC2, OR, and PrP(23-51) bind to the membrane simultaneously (Figure 4C iv). This further indicates that PrP has three binding sites with lipid membranes.

Studies by using small PrP peptides have shown that the CC1(PrP(23-28)) and CC2(PrP(95-110)) are critical for PrP-lipid interactions[18, 23, 37]. In the research by Boland and coworkers[26], the binding ability of PrP(23-50), PrP(23-89), PrP(23-110), PrP(23-110, PrP(50-110), PrP(51-89), and PrP(90-110) to lipid membrane were investigated. However, only the PrP(23-89) and PrP(23-110) have interactions with the lipid membrane. In their study, PrP(23-50), PrP(51-89), PrP(50-110), parts of the PrP(23-89) and PrP(23-110) do not have interactions with lipid membrane. This result may suggest that combination of the subdomains is needed for effective membrane interaction. To date, however, the lipid-interacting regions in full-length PrP and their corresponding force values are ill-defined. In our study, by analyzing the unbinding distance, three binding regions in PrP are well defined. The CC2 has interactions with lipid membrane with force peak at about 89.7±2.7 pN (Figure 3E). The binding of OR to our man-made lipid membranes may happen through the interaction between the tryptophan residues and the acyl chain region of the membrane[25], and the force for this interaction is 98.7±3.0 pN (Figure 3D). Figure 3F indicates that the unbinding force of PrP(23-51) to lipid membrane (corresponding to the third peak of unbinding distance) is the strongest of the three, with a force value of 139.7±8.7 pN, and the binding probability is the smallest (Figure 3C). It has been suggested that the N2 (PrP(23-89)) fragment has strong interactions with lipid membrane by inserting into the lipid bilayer in a minimally disruptive manner rather than associating with the membrane surface, and a number of studies show that the insertion of peptide into lipid membrane encounters significant energy barriers[40, 41], which explains why the PrP(23-51) has the strongest interaction with lipid membrane while the binding probability is the lowest.

Spectroscopic data suggests that the binding of PrP to lipid membrane results in a significant increase of ordering in the N-terminal part of the molecule, which is related to the structure conversion of PrP[11]. However, the exact mechanism of this ordering of the N-terminal part is unclear. In order to further understand the effect of PrP-lipid interactions on PrP's conformational change, we use molecular dynamics (MD) methods to predict the structure of the full-length PrP (Figure 1). The MD simulation shows that the N-terminal of PrP is disordered and dynamic in solution. Our single molecule studies show that the fragments CC2, OR, and PrP(23-51) of the PrP polypeptide folding structure bind to lipid membranes (ESI Figure S3 †). This interaction should highly reduce the flexibility of the N-terminal of PrP. Combining SMFS and MD provides new insight into the mechanism of PrP structure conversion after its binding to lipid membrane.

Conclusions

Two different functionalization methods suggest that PrP was modified on the AFM tip through the sulfur atoms of a disulfide formed between Cys179 and Cys214. The advantage of this functionalization is that the exact location attached to the AFM tip is exclusively defined. Using this method, we modified the AFM tip with PrP and investigated the interactions between the PrP and lipid membrane. Analysis of the unbinding distances revealed that the PrP has three main binding regions with lipid membrane, of which the corresponding binding forces were acquired. Combining the force distance two-dimensional histogram and the worm-like chain simulation curves, the exact lipid-interacting regions in PrP and their corresponding binding forces are visualized, which also provides a new approach for investigating the binding domains in protein.

Conflicts of interest

"There are no conflicts to declare".

Acknowledgements

This work was supported in part by US National Science Foundation (ECCS 1609788).

Notes and References

1. J. C. Sigurdson, C. J. Bartz and M. Glatzel, *Annu Rev Pathol-Mech*, 2019, **14**, 497-516.
2. S. B. Prusiner, *Proceedings of the National Academy of Sciences*, 1998, **95**, 13363-13383.
3. S. B. Prusiner, *Science (New York, N.Y.)*, 1982, **216**, 136-144.
4. H. J. Dyson and P. E. Wright, *Nature reviews. Molecular cell biology*, 2005, **6**, 197-208.
5. D. Gajdusek, *Science (New York, N.Y.)*, 1977, **197**, 943-960.
6. N. Stahl, D. R. Borchelt, K. Hsiao and S. B. Prusiner, *Cell*, 1987, **51**, 229-240.
7. J. Brettschneider, K. D. Tredici, V. M. Y. Lee and J. Q. Trojanowski, *Nature Reviews Neuroscience*, 2015, **16**, 109.
8. D. N. Dean, P. Rana, R. P. Campbell, P. Ghosh and V. Rangachari, *Biophys J*, 2018, **114**, 539-549.
9. J. Rasmussen, M. Jucker and L. C. Walker, *Prion*, 2017, **11**, 215-225.
10. H. Eraña, *Prion*, 2019, **13**, 41-45.
11. M. Morillas, W. Swietnicki, P. Gambetti and W. K. Surewicz, *The Journal of biological chemistry*, 1999, **274**, 36859-36865.
12. S. Srivastava and I. V. Baskakov, *PLoS ONE*, 2015, **10**, e0130283.
13. J. Ma, *PLoS Pathogens*, 2012, **8**, e1002589.
14. F. Wang, F. Yang, Y. Hu, X. Wang, X. Wang, C. Jin and J. Ma, *Biochemistry*, 2007, **46**, 7045-7053.

15. X. Wang, F. Wang, L. Arterburn, R. Wollmann and J. Ma, *The Journal of biological chemistry*, 2006, **281**, 13559-13565.
16. C. L. Haigh, S. C. Drew, M. P. Boland, C. L. Masters, K. J. Barnham, V. A. Lawson and S. J. Collins, *Journal of cell science*, 2009, **122**, 1518-1528.
17. C. L. Haigh, V. A. Lewis, L. J. Vella, C. L. Masters, A. F. Hill, V. A. Lawson and S. J. Collins, *Cell research*, 2009, **19**, 1062-1078.
18. C. L. Haigh, C. Tumpach, S. C. Drew and S. J. Collins, *Plos One*, 2015, **10**.
19. V. Rangachari, N. D. Dean, P. Rana, A. Vaidya and P. Ghosh, *BBA-BIOMEMBRANES*, 2018, **1860**, 1652-1662.
20. A. Aguzzi and A. M. Calella, *Physiological reviews*, 2009, **89**, 1105-1152.
21. R. Zahn, A. Liu, T. Luhrs, R. Riek, C. von Schroetter, F. Lopez Garcia, M. Billeter, L. Calzolai, G. Wider and K. Wuthrich, *Proceedings of the National Academy of Sciences of the United States of America*, 2000, **97**, 145-150.
22. L. L. P. Hosszu, N. J. Baxter, G. S. Jackson, A. Power, A. R. Clarke, J. P. Waltho, C. J. Craven and J. Collinge, *Nat Struct Mol Biol*, 1999, **6**, 740-743.
23. F. Wang, S. Yin, X. Wang, L. Zha, M.-S. Sy and J. Ma, *Biochemistry*, 2010, **49**, 8169-8176.
24. A. P. Le Brun, C. L. Haigh, S. C. Drew, M. James, M. P. Boland and S. J. Collins, *Biophys J*, 2014, **107**, 2313-2324.
25. S. L. Dong, S. A. Cadamuro, F. Fiorino, U. Bertsch, L. Moroder and C. Renner, *Biopolymers*, 2007, **88**, 840-847.
26. M. P. Boland, C. R. Hatty, F. Separovic, A. F. Hill, D. J. Tew, K. J. Barnham, C. L. Haigh, M. James, C. L. Masters and S. J. Collins, *The Journal of biological chemistry*, 2010, **285**, 32282-32292.
27. Y. Sun, W.-C. Hung, M.-T. Lee and H. W. Huang, *Biochimica et Biophysica Acta (BBA) - Biomembranes*, 2015, **1848**, 2422-2429.
28. M. S. Khan, N. S. Dosoky and J. D. Williams, *International Journal of Molecular Sciences*, 2013, **14**, 21561-21597.
29. C. Rankl, F. Kienberger, L. Wildling, J. Wruss, H. J. Gruber, D. Blaas and P. Hinterdorfer, *Proceedings of the National Academy of Sciences of the United States of America*, 2008, **105**, 17778-17783.
30. B. Wang, C. Guo, Z. Lou and B. Xu, *Chemical Communications*, 2015, **51**, 2088-2090.
31. R. Nevo, C. Stroh, F. Kienberger, D. Kaftan, V. Brumfeld, M. Elbaum, Z. Reich and P. Hinterdorfer, *Nature structural biology*, 2003, **10**, 553-557.
32. G. van Meer, *Annual review of cell biology*, 1989, **5**, 247-275.
33. R. Zhu, S. Howorka, J. Proll, F. Kienberger, J. Preiner, J. Hesse, A. Ebner, V. P. Pastushenko, H. J. Gruber and P. Hinterdorfer, *Nat Nano*, 2010, **5**, 788-791.
34. C. He, C. Hu, X. Hu, X. Hu, A. Xiao, T. T. Perkins and H. Li, *Angewandte Chemie International Edition*, 2015, **54**, 9921-9925.
35. M. Rief, M. Gautel, F. Oesterhelt, J. M. Fernandez and H. E. Gaub, *Science (New York, N.Y.)*, 1997, **276**, 1109-1112.
36. L. J. Lapidus, P. J. Steinbach, W. A. Eaton, A. Szabo and J. Hofrichter, *The Journal of Physical Chemistry B*, 2002, **106**, 11628-11640.
37. M. Béland and X. Roucou, *Journal of Neurochemistry*, 2012, **120**, 853-868.
38. D. A. Harris, M. T. Huber, P. van Dijken, S. L. Shyng, B. T. Chait and R. Wang, *Biochemistry*, 1993, **32**, 1009-1016.
39. S. G. Chen, D. B. Teplow, P. Parchi, J. K. Teller, P. Gambetti and L. Autilio-Gambetti, *The Journal of biological chemistry*, 1995, **270**, 19173-19180.
40. M. Hong and Y. Su, *Protein science : a publication of the Protein Society*, 2011, **20**, 641-655.
41. M. W. Maddox and M. L. Longo, *Biophysical Journal*, 2002, **82**, 244-263.
42. W. Swietnicki, R. Petersen, P. Gambetti and W. K. Surewicz, *The Journal of biological chemistry*, 1997, **272**, 27517-27520.

TOC

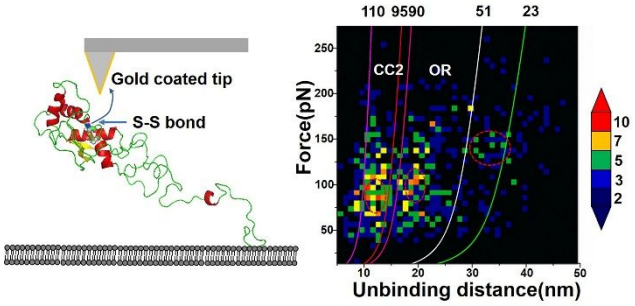

GRAPHICAL AND TEXTUAL ABSTRACT

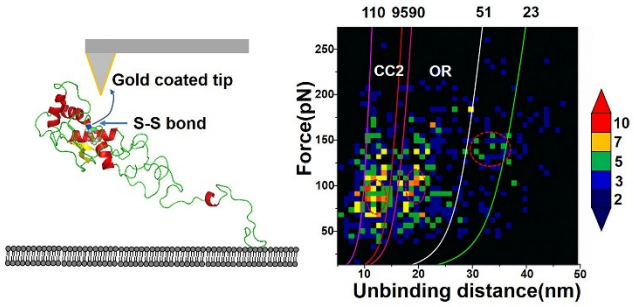

A new method combining AFM measurements and molecular modeling was used to unravel the molecular basis of interaction domains of full-length PrP with lipid membrane.